RSC Advances

PAPER

View Article Online
View Journal | View Issue

Published on 07 January 2016. Downloaded by Xian Jiaotong University on 11/08/2016 08:26:43.

Cite this: *RSC Adv.*, 2016, **6**, 7610

Preparation and characterization of titanium-based PbO_2 electrodes modified by ethylene glycol

Xu Hao,[a] Guo Wuqi,[a] Wu Jia,[a] Feng Jiangtao,*[a] Yang Honghui[ab] and Yan Wei*[ab]

Received 13th October 2015
Accepted 4th January 2016

DOI: 10.1039/c5ra21195f

www.rsc.org/advances

The present work focused on studying the effect of ethylene glycol (EG) modification on the electrochemical properties of lead dioxide electrodes prepared by the electrochemical deposition method. The surface morphology and the structure of the electrodes were characterized by scanning electronic microscopy (SEM) and X-ray diffraction (XRD), respectively. The stability and electrochemical activity of lead dioxide electrodes were investigated by the accelerated life test, linear sweep voltammetry, cycle voltammetry and simulated wastewater degradation. The results showed that EG significantly decreased the grain size of lead dioxide and resulted in the formation of a compact and uniform surface coating. The electrode prepared from the solution containing 2.5 vt% EG (marked as the PbO_2-EG (2.5 vt%) electrode) showed the longest service life (212.6 h). During the electrochemical characterization analysis, the PbO_2-EG (2.5 vt%) electrode showed the highest electrochemical degradation capacity, which could be attributed to its highest relative roughness factor, the highest voltammetric charge quantity and the highest oxygen evolution potential. Consequently, the PbO_2-EG (2.5 vt%) electrode showed the best performance on degradation of Acid Red G (the highest removal efficiency and the lowest energy consumption) in simulated wastewater by bulk electrolysis.

1 Introduction

The electrochemical degradation method is an effective approach for treating toxic or bio-refractory organic pollutants on account of its prominent oxidation performance, ease of operation and environmental compatibility.[1–3] For application of the electrochemical degradation method, appropriate electrodes with high electrochemical activity and long service life are essential.[4] The degradation efficiency and mineralization degree are strongly dependent on the properties of the selected electrode. Up to date, various types of electrodes including Pt, graphite, boron doped diamond (BDD),[5] IrO_2,[6] RuO_2,[7] SnO_2 (ref. 8) and PbO_2 have been widely investigated.

Among of them, PbO_2 was regarded as the optimum anodic materials in applications for the wastewater purification due to its superior integrated performances, including high chemical stability in corrosive media, relatively high over-potential in oxygen evolution reactions and low price compared with noble metal electrodes.[9] Therefore, PbO_2 anode materials have attracted more and more attention in the field of electrochemical degradation treatment. For instance, PbO_2 anode has been employed to oxidize recalcitrant organic pollutants such as real landfill leachate,[10] dimethyl phthalate,[11] trichlorophenoxyacetic acid,[12] lignin,[13] levodopa[14] and tebuconazole pesticide[15] by ·OH produced during water electrolysis as shown in eqn (1) and (2).

$$PbO_2 + H_2O \rightarrow PbO_2(\cdot OH) + H^+ + e \quad (1)$$

$$R + \cdot OH \rightarrow \text{intermediate} \rightarrow CO_2 + H_2O \quad (2)$$

Many efforts has been paid on modification of the PbO_2 electrode for further improvement of its performance in the electrochemical degradation of organic pollutants in water.[16] The first approach for PbO_2 modification is to improve the preparation method of PbO_2 electrodes, such as using the pulse electro-deposition method[17,18] or using a novel deposition solution containing methanesulfonic acid.[19,20] The second way is to use some new materials to replace conventional titanium plate as the substrates. For example, some researchers used TiO_2 nanotube arrays as the substrate to fabricate a novel three-dimensional PbO_2 electrode.[21–24] The third method is to modify the PbO_2 layer by adding some modification materials into the electrochemical deposition solution. A frequently-used materials are some cations (such as Bi^{2+},[25,26] Fe^{3+},[24,27] Ce^{2+},[28–30] Zr^{4+},[17,31,32] Cu^{2+},[33] Pr^{3+} (ref. 34) and La^{2+} (ref. 35)) and anions (such as $[Fe(CN)_6]^{3-}$ (ref. 3) and F^- (ref. 11 and 36–38)). Meanwhile, the electrochemical oxidation ability and stability of PbO_2 electrode can also be enhanced by some non-ion materials, such as carbon nanotubes,[39–41] ionic liquids,[42] polyethylene glycol (PEG),[43] polytetrafluoroethylene (PTFE)[35,37,44] and polyvinylpyrrolidone (PVP).[45]

[a]*Department of Environmental Science and Engineering, Xi'an Jiaotong University, Xi'an, 710049, P. R. China. E-mail: fjtes@mail.xjtu.edu.cn; yanwei@mail.xjtu.edu.cn*
[b]*The State Key Laboratory of Multiphase Flow in Power Engineering, Xi'an Jiaotong University, Xi'an, 710049, P. R. China*

This journal is © The Royal Society of Chemistry 2016

Published on 07 January 2016. Downloaded by Xian Jiaotong University on 11/08/2016 08:26:43.

To the best of our knowledge, there is no report in using different solute to modify PbO_2 electrode by electrochemical deposition method. Therefore, in the present work, for the sake of studying the effect of ethylene glycol (EG) modification, Ti/SnO_2–Sb/α-PbO_2/β-PbO_2 electrodes were fabricated by electrochemical deposition with EG in the deposition solution. The morphology, crystalline structures, the relative roughness factor, oxygen evolution potential, voltammetric charge quantity and electrochemical stability of the as-prepared electrode were characterized. In order to evaluate its electro-catalytic activity, Acid Red G (ARG, $C_{18}H_{13}N_3Na_2O_8S_2$, CAS number: 3734-67-6) was employed as the toxic bio-refractory model organic pollutant for electrochemical degradation.

2 Materials and experiment

2.1 Materials

All chemicals used in the experiment were of analytical reagent grade or higher and were used as received. The titanium (Ti) plate (purity: 99.6%, BaoTi Co. Ltd, China) with 0.5 mm-thickness was used in this study. Deionized water prepared from an EPET-40TF system (EPET Co. Ltd, Nanjing, China) was used for aqueous solution preparation and Ti plate washing.

2.2 Electrode preparation

Ti plates with a dimension of 2 cm × 5.0 cm × 0.5 mm were used as the electrode substrate. The pre-treatment of Ti plate and the preparation of the inner layer (the thermal deposition process of Sb–SnO_2 layer and the electrochemical deposition process of α-PbO_2 layer) were the same as our previous work.[3,27,33]

The surface β-PbO_2 layer was coated on the Ti/Sb–SnO_2/α-PbO_2 electrode through the electrochemical deposition process. The deposition solution was composed of 0.5 mol L^{-1} $Pb(NO_3)_2$, 0.01 mol L^{-1} NaF, 0.2 mol L^{-1} $Cu(NO_3)_2$ and water/EG. The solution pH was adjusted to 2.0 using concentrated HNO_3. The deposition processes were carried out at 65 °C for 120 min and the current density was controlled at 10 mA cm^{-1}. The copper plate with the same size was used as the counter cathode. EG was added into the electrochemical deposition solution with fixed amounts. The fabricated electrodes were marked as PbO_2-EG (0 vt%), PbO_2-EG (1.0 vt%), PbO_2-EG (2.5 vt%) and PbO_2-EG (5.0 vt%), respectively, which was dependent on different EG volume fractions of the solution for electrode fabrication.

2.3 Characterization analysis

The morphology of samples was characterized by scanning electron microscopy (SEM, JEOL, JSM-6390A). X-ray diffraction (XRD, D/MAX-2400X, Rigaku) analysis was performed using a diffractometer with Cu-K_α radiation with the accelerating voltage of 40 kV and the electron probe current of 40 mA.

Electrochemical measurements were carried out on the CHI 660D electrochemical workstation (Shanghai Chenhua Instrument Co. Ltd., China) with a conventional three-electrode cell at room temperature. The as-prepared PbO_2 electrode served as the working electrode, while the Pt sheet served as the counter electrode and the Ag/AgCl/saturated KCl electrode as the reference electrode. Linear sweep voltammetry was performed in 0.5 mol L^{-1} Na_2SO_4 solution at 50 mV s^{-1} in the range of 0.6–2.0 V. Cyclic voltammograms were recorded at different scan rates, in 0.5 M Na_2SO_4 aqueous solutions and in a selected potential region between 0.6 and 1.3 V *vs.* Ag/AgCl/saturated KCl, where only double layer charging currents were observed. The results were used to calculate the relative roughness factor.[46] Cycle voltammetry curves were recorded between 0 and 2 V in 0.5 mol L^{-1} H_2SO_4 solution at different scan rates and the results were used to calculate the voltammetric charge quantity for different electrodes.

Anti-corrosion performance of the electrodes was investigated by accelerated lifetime test with a current density of 500 mA cm^{-2} in 3 mol L^{-1} H_2SO_4 solution. Temperature of the sulfuric acid solution was kept at 45 °C ± 2 °C by the electrical resistance heating. During the accelerated lifetime test, the cell voltage was measured automatically by the electrochemical workstation and the test was considered to be end when the cell voltage was higher than 10 V.

2.4 Electrochemical oxidation

The bulk electrochemical oxidation tests were conducted in batch using an undivided electrolytic cell under galvanostatic conditions. The current density of 5.0 mA cm^{-2} was supplied by a WYK-303B potentiostat/galvanostat. The prepared electrodes served as the anodes and the cathode was stainless steel sheets (2.0 cm × 5.0 cm) with a distance of 2.0 cm between the two electrodes. The initial ARG concentration was 100 mg L^{-1} and 0.5 mol L^{-1} Na_2SO_4 was added to the aqueous solution as the supporting electrolyte. Experiments were carried out at room temperature for 120 min. During the experiments, liquid samples were withdrawn from the electrolytic cell every 20 min for the HPLC and total organic carbon (TOC) analysis. Each degradation process was repeated for three times and the average values were used for the electrochemical oxidation performance analysis.

The water HPLC system (515 HPLC pump, 2489 UV/visible detector and 717 plus auto-sampler) was used to identify organic compounds with an ACE 5 C18 column (250 × 4.6 mm). The composition of the mobile phase was 80% acetonitrile and 20% acetic acid (20 mL acetic acid in 1000 mL deionized water). The flow rate was 0.8 mL min^{-1} and the UV-vis detector was set at 503 nm. The retention time of the probe in this condition was 2.8 min. The ARG concentration (C, mg L^{-1}) was calculated from the probe peak area with the standard curve. The ARG removal efficiency (η_{ARG}, %) was calculated as follow,

$$\eta_{ARG} = \frac{C_0 - C_t}{C_0} \times 100\% \quad (3)$$

where C_0 is the initial concentration of ARG and C_t is the ARG concentration at given time t.

The TOC value (mg L^{-1}) of the water sample was determined by a Shimadzu TOC 5000A apparatus. The TOC removal efficiency (η_{TOC}, %) was calculated as follow,

Published on 07 January 2016. Downloaded by Xian Jiaotong University on 11/08/2016 08:26:43.

$$\eta_{TOC} = \frac{TOC_0 - TOC_t}{TOC_0} \times 100\% \quad (4)$$

where TOC_0 is the initial TOC concentration and TOC_t is the TOC concentration value at given time t.

The TOC energy consumption (EC_{TOC}, kW h g_{TOC}^{-1}) was calculated as follow,

$$EC_{TOC} = \frac{50}{3} \frac{I \int U_{cell} dt}{\Delta TOC V} \quad (5)$$

where U_{cell} is the cell voltage (V), I is the current during the reaction (A), t is the electrolysis time (min), V is the volume of the treated solution (mL) and ΔTOC is the TOC-removal value during the electrochemical degradation process (mg L^{-1}).

3 Results and discussion

3.1 Surface analysis of PbO_2 electrodes

3.1.1 SEM analysis. Fig. 1 shows the SEM micrographs of the PbO_2 electrodes prepared with different EG volume fractions. Fig. 1a displays the morphology of the surface layer of the PbO_2-EG (0 vt%) electrode was uniform and of typical pyramidal shape with obvious boundaries, which was similar to the earlier reports.[3,11,18,33,45,47] There were considerable fractions of areas (*i.e.* black spots) that were not fully covered by PbO_2 as shown in the inset of Fig. 1a. After EG was added into the deposition solution as modification materials, some changes were observed on PbO_2 electrode surface. As shown in Fig. 1b, PbO_2-EG (1.0 vt%) electrodes lost the pyramidal shape and the particle size was slightly diminished compared with that of the PbO_2-EG (0 vt%) electrode. An increase in the volume fraction of EG to 2.5 vt% caused a pronounced change in the morphology of prepared electrodes. As it is seen from Fig. 1c, a well-defined structure consisting of globular shape particles was formed.[33,43,47] A further increase in EG to 5.0 vt% (Fig. 1d) resulted in a uniform structure consisting of a pileup-pellets pattern with non-distinguishable boundaries and the smallest globular particles, which was similar to earlier reports.[43,45,48]

It can be found that the PbO_2-EG (2.5 vt%) electrode had the most smooth surface in the four electrodes as shown in the insets of Fig. 1. It can be hypothesized that increment of the EG volume fraction in the electrochemical deposition solution could significantly reduce the particle size of PbO_2 crystals and obtain a compact and fine coating surface.

3.1.2 XRD. Fig. 2 shows XRD patterns of the PbO_2 electrodes with different EG volume fractions. The main diffraction peaks of the PbO_2-EG (0 vt%) electrode at 32.0° and 49.0° were assigned to the (101) and (211) plane of β-PbO_2, respectively. When EG was introduced into the electrochemical deposition solution, there was no difference of the crystalline orientation for the prepared PbO_2-EG (1.0 vt%) and PbO_2-EG (2.5 vt%) electrodes. However, the main peaks intensity of PbO_2-EG (1.0 vt%) and PbO_2-EG (2.5 vt%) electrodes was higher than that of PbO_2 (0 vt%). As the EG volume fraction increased to 5.0 vt%, a new diffraction peak appeared at 36.2° which was assigned to the β (200) plane. It can be seen from Fig. 2 that EG modification could widen PbO_2 diffraction peaks. The average grain sizes of PbO_2 crystals of electrodes were calculated using the Debye–Scherrer equation:

$$D = \frac{k\lambda}{\beta \cos \theta} \quad (6)$$

where D is the crystallite size, λ is the X-ray wavelength, β is the full width at half maximum of the peak and θ is the diffraction angle.

The results were shown in Table 1. It can be found that the crystal size of PbO_2 electrodes reduced with the increase of the EG volume fraction, which was consistent with SEM morphology in Fig. 1. These results suggested that the increment of the EG volume fraction decreased the grain size of lead dioxide electrodes.

Thus, from the results obtained, it can be concluded that EG played two different roles in the process of PbO_2 electrodeposition. First, EG molecules could surround the deposited PbO_2 particles, restrict their further growth and the particles size was diminished.[45] Second, it seems that the surface diffusion of ad-atoms might be facilitated in the presence of EG and

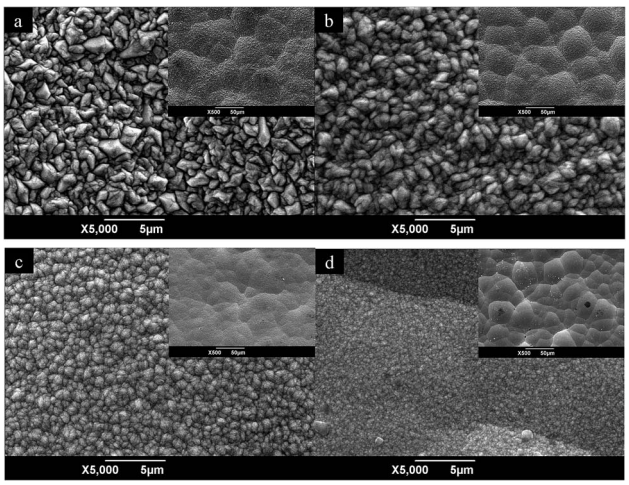

Fig. 1 SEM photographs of the PbO_2 electrodes with different EG amounts ((a) 0 vt%, (b) 1.0 vt%, (c) 2.5 vt%, (d) 5.0 vt%).

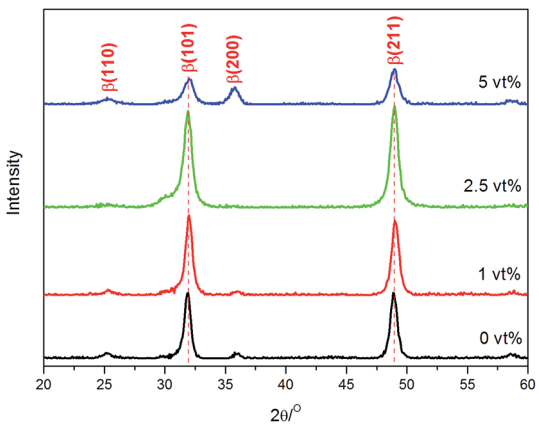

Fig. 2 XRD patterns of the PbO_2 electrodes with different EG concentration.

This journal is © The Royal Society of Chemistry 2016

Published on 07 January 2016. Downloaded by Xian Jiaotong University on 11/08/2016 08:26:43.

Table 1 Various characterization parameters for different PbO_2 electrodes modification with EG

	PbO_2-EG (0 vt%)	PbO_2-EG (1 vt%)	PbO_2-EG (2.5 vt%)	PbO_2-EG (5 vt%)
Crystal size/nm	13.5	13.0	11.3	10.4
Relative roughness factor	39	63	64.3	53.8
Oxygen evolution potential/V	1.498	1.587	1.612	1.610
Current density at 2.0 V/mA cm^{-2}	4.85	3.25	8.46	3.08
Accelerated test life/h	100	163	212	74
Average loading amount/mg cm^{-2}	34.9	31.0	28.3	19.9

hence the creation of excess nuclei was suppressed. Consequently, a more homogeneous distribution of current at the electrode/electrolyte interface occurred. Under such conditions, the process of PbO_2 electro-deposition took place at slower rates which enabled the species to find the most suitable positions in the structure.

3.2 Electrochemical analysis of PbO_2 electrodes

3.2.1 Relative roughness factor. The relative roughness factor reflecting the real surface area of electrodes is defined as real surface area per apparent geometric area of electrodes and calculated through comparing determined capacitance with the capacitance of a smooth oxide surface (60 mF cm^2).[4,46,49] From the cyclic voltammogram results mentioned in Section 2.3, I values for different scan rates were obtained at $E = 1.0$ V *vs.* Ag/AgCl/saturated KCl, a point where an approximate symmetry of anodic and cathodic currents was observed. The linear relationship between current density and sweep rates confirmed the non-faradic character of the current in this potential region.[46] The capacitances were obtained from plot slopes in Fig. 3 and were compared with the value of 60 mF cm^2 to estimate the roughness factor. As shown in Table 1, the relative roughness factor increased as the following order of PbO_2-EG (0 vt%), PbO_2-EG (5.0 vt%), PbO_2-EG (1.0 vt%) and PbO_2-EG (2.5 vt%). From Fig. 1 and Table 1, one can find that the PbO_2 crystal size decreased with the increase of EG concentration. The decrease of crystal size means the number of PbO_2 crystal in every apparent geometric area of electrodes increased. This made the relative roughness factor increase under the EG modification. Thus, the introduction of EG could improve the roughness of

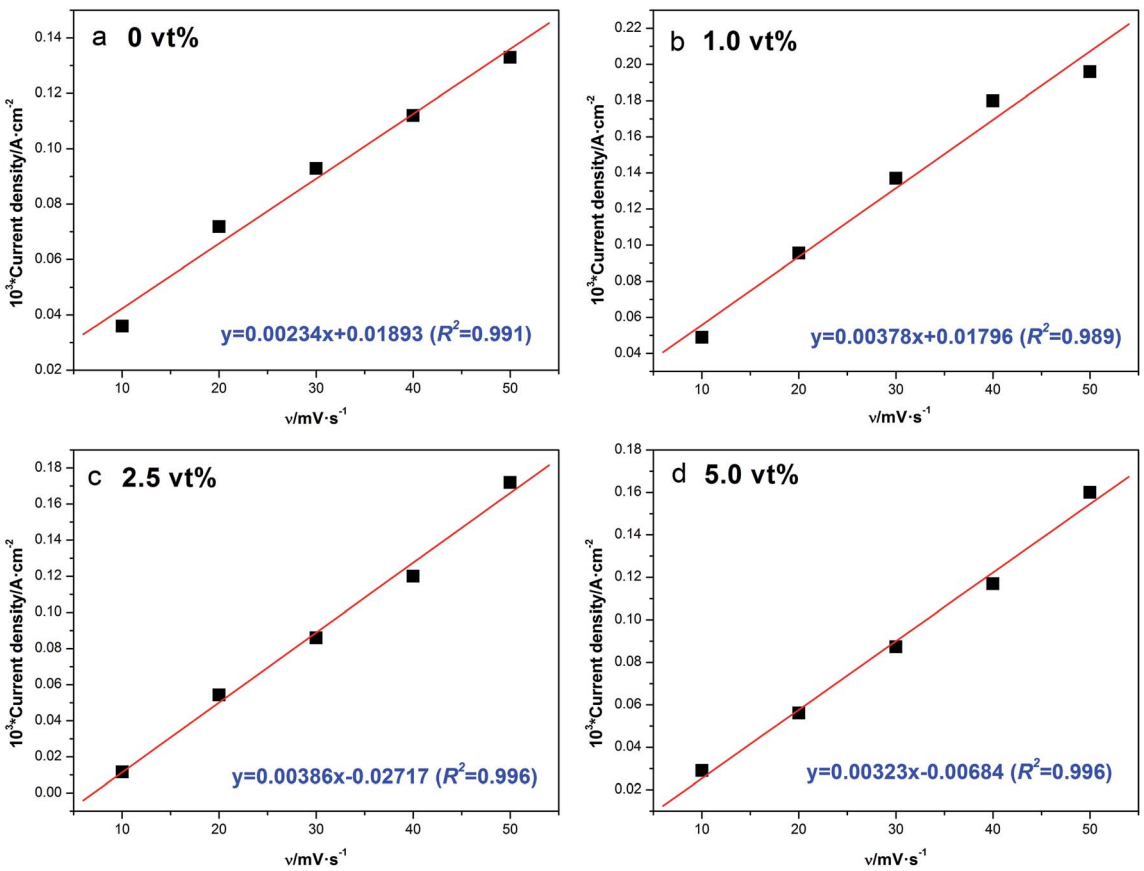

Fig. 3 Linear regression between I and the different sweep rates, measured at 1.0 V (*vs.* Ag/AgCl/saturated KCl), ((a) 0 vt%, (b) 1.0 vt%, (c) 2.5 vt%, (d) 5.0 vt%).

Published on 07 January 2016. Downloaded by Xian Jiaotong University on 11/08/2016 08:26:43.

PbO_2 electrode surface. This may be favorable for the electrocatalytic activity of PbO_2 electrode.

3.2.2 Linear sweep voltammograms. Fig. 4 shows the linear sweep voltammograms of PbO_2 electrodes in 0.5 mol L^{-1} Na_2SO_4 solution at a scan rate of 20 mV s^{-1}. As shown in Table 1, the oxygen evolution potential increased as the following order of PbO_2-EG (0 vt%), PbO_2-EG (1.0 vt%), PbO_2-EG (5.0 vt%) and PbO_2-EG (2.5 vt%). This indicated that the introduction of EG into the electrochemical deposition solution increased the oxygen evolution potential of the modified PbO_2 electrodes. The high oxygen evolution over potential is desired since oxygen evolution is a competitive reaction in the process of anodic oxidation of pollutants.[3] The highest over potential for oxygen evolution of the PbO_2-EG (2.5 vt%) electrode indicated the performance of this electrode was higher than that of other PbO_2 electrodes on organics degradation.

In addition to that, it can be noted that conductivities of PbO_2 electrodes were different. For instance, the current density were 4.85, 3.25, 8.46 and 3.08 mA cm^{-2} for PbO_2-EG (0 vt%), PbO_2-EG (1.0 vt%), PbO_2-EG (2.5 vt%) and PbO_2-EG (5.0 vt%), respectively. This indicated that the PbO_2-EG (2.5 vt%) electrode posed the highest conductivity, which could benefit the saving of energy consumptions.

3.2.3 Voltammetric charge quantity. The electrochemical activity was related to real surface area and the number of active sites accessible to the electrolyte.[49] The voltammetric charge quantity (q^*), which is related to real surface area and the number of active sites, can reflect the electrochemical activity of an electrode.[8] For the same electrode material, larger q^* indicates higher electrode activity.[50] The method reported in literature[4,8,49,50] was employed to calculate q^* for estimating the electrode activity. The q^* was obtained by integration of the cycle voltammetric curves over the whole potential range from 0 to 2 V. Fig. 5 shows the relationship of q^* against the reciprocal of the square root of scan rates for different PbO_2 electrodes. The PbO_2-EG (2.5 vt%) electrode exhibits the highest q^* values, followed by PbO_2-EG (1.0 vt%) and then PbO_2-EG (0 vt%), PbO_2-EG (5.0 vt%). The results indicated that the PbO_2-EG (2.5 vt%) electrode showed the highest voltammetric charge quantity q^*. With the results shown in Fig. 3 and 5, it could be concluded that the PbO_2-EG (2.5 vt%) electrode had the highest active surface area. Meanwhile, the q^* value of PbO_2-EG (5.0 vt%) was very similar to that of PbO_2-EG (0 vt%), which indicated that the active surface area and the number of active sites of the two kinds of electrodes were similar.

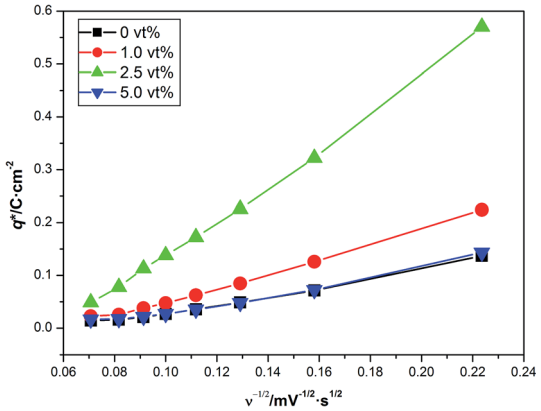

Fig. 5 Relationship of voltammetric charge quantity (q^*) *versus* the reciprocal of square root of scan rate in 0.5 mol L^{-1} H_2SO_4 solution.

3.2.4 Electrochemical stability test. Fig. 6 shows the time course of cell potential in the accelerated life test for different PbO_2 electrodes under 3 mol L^{-1} H_2SO_4 solution with a current density of 500 mA cm^{-2}. According to Fig. 6, it was observed that the EG modification could obviously extend the lifetime of PbO_2 electrodes until the EG volume fraction was up to 5.0%. Considering that the electrode was deactivated when the cell potential increased to 10 V, the PbO_2-EG (2.5 vt%) electrode displayed the longest lifetime (212.6 h), followed by the PbO_2-EG (1.0 vt%) electrode (163.5 h), the PbO_2-EG (0 vt%) electrode (101 h) and the PbO_2-EG (5.0 vt%) electrode (74 h). Compared with our previous work, it can be found that the accelerated lifetime of PbO_2-EG (2.5 vt%) was longer than that of the PbO_2–Cu (0.2 M) electrode.[33]

The reason for the longer accelerated life of PbO_2-EG (1.0 vt%) and PbO_2-EG (2.5 vt%) was the dense microstructure

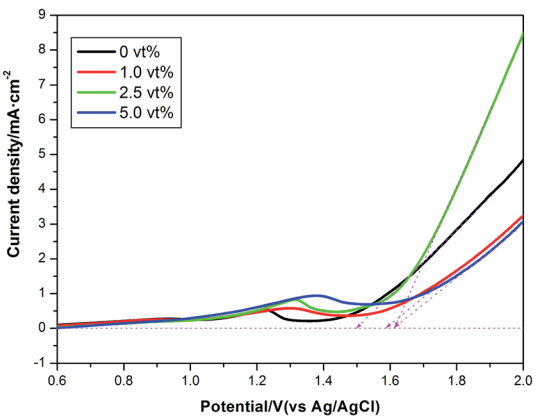

Fig. 4 Linear sweep voltammograms curves of different PbO_2 electrodes in 0.5 mol L^{-1} H_2SO_4 solution, scan rate: 20 mV s^{-1}.

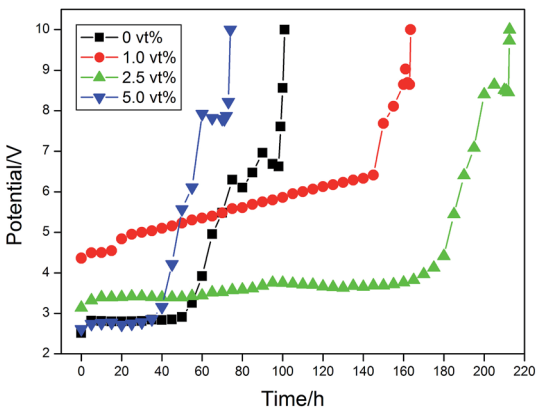

Fig. 6 Variation of cell potential with time in the accelerated life test for different PbO_2 electrodes.

This journal is © The Royal Society of Chemistry 2016

Published on 07 January 2016. Downloaded by Xian Jiaotong University on 11/08/2016 08:26:43.

of EG modified electrodes. As shown in Fig. 1 and Table 1, the decrease of PbO_2 particle size could reduce the defect density of electrode surface and make a compact and fine surface layer.[33] The compact surface of EG modified PbO_2 electrodes could not only baffle the penetration of the electrolyte through cracks and pores, but also prevent an increase of pressure inside the electrode caused by the internal O_2 evolution.[32] Thus, the probability of mechanical ruptures of the electrode was diminished, which resulted in the high electrochemical stability showed by the PbO_2-EG (1.0 vt%) and PbO_2-EG (2.5 vt%) electrodes. However, the average loading amount of the PbO_2-EG (5.0 vt%) electrode was 19.9 mg cm^{-2}, lower than 34.9 mg cm^{-2} of the PbO_2-EG (0 vt%) electrode. The deactivation of the PbO_2 electrode is due to dissolution, detachment and passivation of coating.[40] No detachment was observed during the accelerated life test. Thus the electrode deactivation was attributed to dissolution and passivation. From the point of dissolution, a lower loading amount of oxide led to a lower accelerated lifetime,[3] which caused the weaker electrochemical stability expressed by the PbO_2-EG (5.0 vt%) electrode.

3.3 Electrochemical degradation test

To investigate the electro-catalytic degradation activity of the prepared electrodes, the PbO_2 electrodes were used as the anode in the decolorization treatment of aqueous ARG solution and their ability on mineralization was also studied. Curves of ARG removal efficiency with degradation time are shown in Fig. 7a. It is clear from Fig. 7a and Table 2 that the ARG removal rates by almost all the anodes were up to 87% within 120 min. The PbO_2-EG (2.5 vt%) electrode showed the highest activity for ARG removal. According to the good linear correlation between the logarithms values of the concentration and treatment time (as shown in the inset of Fig. 7a), the ARG removal reaction fitted pseudo first-order kinetics and the rate equation for the degradation of ARG could be expressed as follows:

Table 2 Various electrochemical degradation parameters for different PbO_2 electrodes

	PbO_2-EG (0 vt%)	PbO_2-EG (1 vt%)	PbO_2-EG (2.5 vt%)	PbO_2-EG (5 vt%)
η_{ARG}/%	87.5	88.7	90.8	87.1
Standard deviation	0.3	0.02	0.09	0.08
k_{app}/min^{-1}	0.0173	0.0180	0.0197	0.0169
R^2	0.999	0.999	0.999	0.999
η_{TOC}/%	8.23	10.2	10.8	8.10
Standard deviation	0.06	0.1	0.04	0.02
EC_{TOC}/kW h g_{TOC}^{-1}	13.0	11.2	9.26	14.5

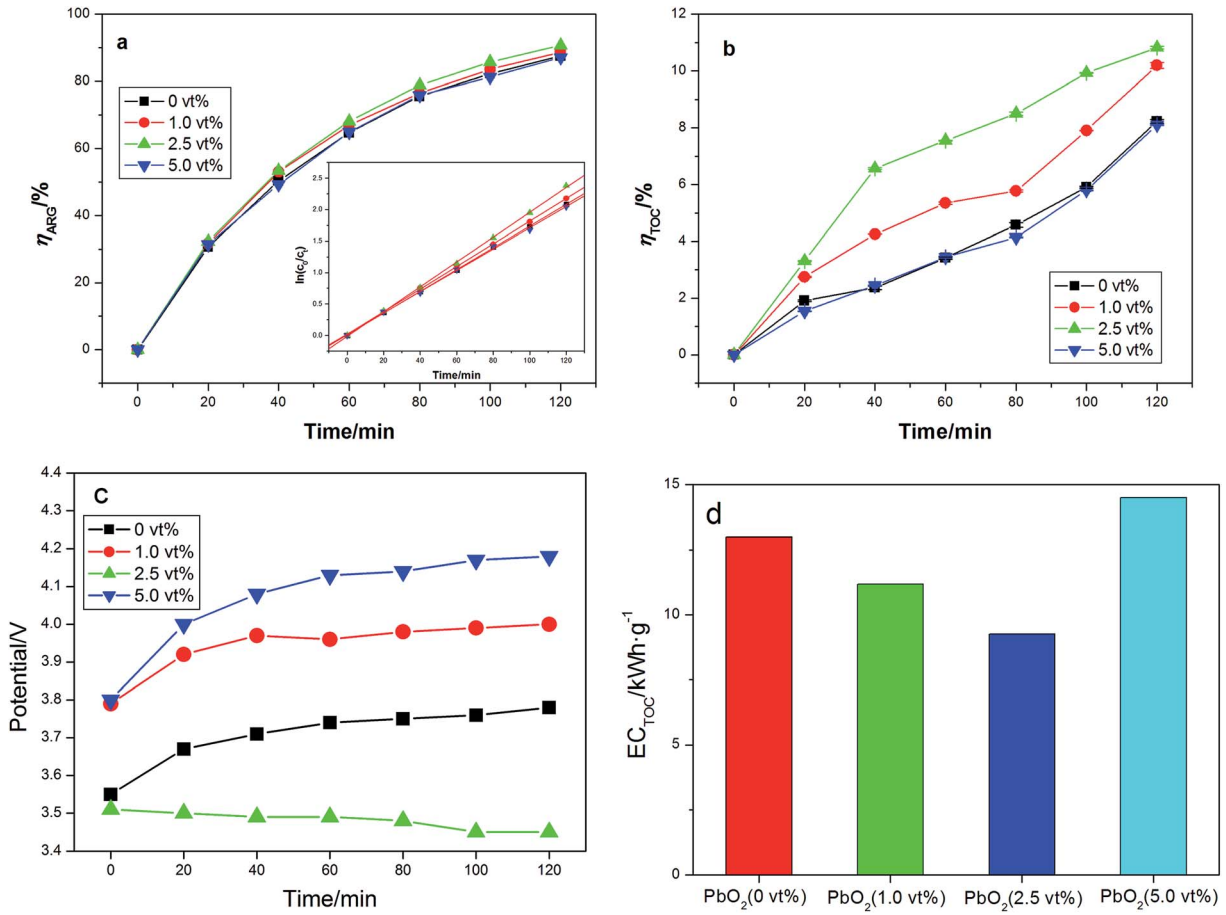

Fig. 7 Variations of (a) the pseudo-first order of ARG decolorization, (b) TOC removal efficiency of ARG degradation, (c) the potential changes *vs.* time curves; (d) EC_{TOC} for different PbO_2 electrodes.

Published on 07 January 2016. Downloaded by Xian Jiaotong University on 11/08/2016 08:26:43.

$$C_t = C_0 e^{-k_{app}t} \quad (7)$$

where k_{app} is the apparent kinetics coefficient.

It is observed in Table 2 that the highest k_{app} value was achieved when the EG volume fraction was 2.5 vt%. Fig. 7b also showed the TOC removal efficiency on these different PbO_2 electrodes during the 120 min degradation process and the PbO_2-EG (2.5 vt%) electrode possessed the highest value of 10.8%. The highest electrochemical degradation capacity for the PbO_2-EG (2.5 vt%) electrode could be ascribed to the highest active surface area and oxygen evolution potential. The PbO_2-EG (2.5 vt%) electrode with larger surface area can provide more active site centers in the gel layer of the coating to generate more ·OH radicals. At the same time, a large surface area of the PbO_2-EG (2.5 vt%) electrode increased the adsorption ability of reagents and ·OH radicals, which resulted in an improvement of electrochemical degradation capacity of PbO_2 anodes.[44]

The electrochemical degradation on these PbO_2 electrodes was performed at the same current density of 5.0 mA cm^{-2} and the cell voltages were monitored during the reaction. As shown in Fig. 7c, the cell voltages increased as the following order of PbO_2-EG (2.5 vt%), PbO_2-EG (0 vt%), PbO_2-EG (1.0 vt%) and PbO_2-EG (5.0 vt%). This result confirmed the conductivity result shown in Fig. 3 that good conductivity and high electrochemical degradation capacity were favorable factors for reducing energy consumptions. As shown in Fig. 7d and Table 2, PbO_2-EG (2.5 vt%) had the lowest energy consumption of 9.26 kW h g_{TOC}^{-1}. On account of the overall pollutant removal performance and the energy consumption, the PbO_2-EG (2.5 vt%) electrode was the best choice among these electrodes, indicating a promising prospect for application.

4 Conclusions

PbO_2 electrodes modified by EG were prepared by the electrodeposition method and used for electrochemical degradation of ARG. EG modification decreased the average grain size of lead dioxide and formed a uniform and compact surface coating. The accelerated life test indicated that the introduction of EG can enhance the stability of PbO_2 electrodes and the PbO_2-EG (2.5 vt%) electrode posed the highest accelerated life (212.6 h). The electrochemical characterization shows that the PbO_2-EG (2.5 vt%) electrode had the highest relative roughness factor, the highest voltammetric charge quantity and the highest oxygen evolution potential, which could benefit its electrochemical degradation capacity. The PbO_2-EG (2.5 vt%) electrode showed the best degradation performance in the simulated wastewater treatment. In summary, the optimization volume fraction of EG obtained for electrochemical deposition of β-PbO_2 coating was 2.5 vt%.

Acknowledgements

The authors gratefully acknowledge the financial support from National Natural Science Foundation of China (No. 21507104).

References

1 B. P. Chaplin, *Environ. Sci.: Processes Impacts*, 2014, **16**, 1182–1203.
2 W. Wu, Z.-H. Huang and T.-T. Lim, *Appl. Catal., A*, 2014, **480**, 58–78.
3 H. Xu, Q. S. Yuan, D. Shao, H. H. Yang, J. D. Liang, J. T. Feng and W. Yan, *J. Hazard. Mater.*, 2015, **286**, 509–516.
4 T. Duan, Y. Chen, Q. Wen and Y. Duan, *RSC Adv.*, 2014, **4**, 57463–57475.
5 M. Haidar, A. Dirany, I. Sirés, N. Oturan and M. A. Oturan, *Chemosphere*, 2013, **91**, 1304–1309.
6 A. T. Marshall and R. G. Haverkamp, *J. Mater. Sci.*, 2012, **47**, 1135–1141.
7 X. Chen and G. Chen, *Electrochim. Acta*, 2005, **50**, 4155–4159.
8 L. Zhang, L. Xu, J. He and J. Zhang, *Electrochim. Acta*, 2014, **117**, 192–201.
9 S. Chai, G. Zhao, Y. Wang, Y.-N. Zhang, Y. Wang, Y. Jin and X. Huang, *Appl. Catal., B*, 2014, **147**, 275–286.
10 M. Panizza and C. A. Martinez-Huitle, *Chemosphere*, 2013, **90**, 1455–1460.
11 F. L. Souza, J. M. Aquino, K. Irikura, D. W. Miwa, M. A. Rodrigo and A. J. Motheo, *Chemosphere*, 2014, **109**, 187–194.
12 D. Maharana, Z. Xu, J. Niu and N. N. Rao, *Chemosphere*, 2015, **136**, 145–152.
13 D. Shao, J. Liang, X. Cui, H. Xu and W. Yan, *Chem. Eng. J.*, 2014, **244**, 288–295.
14 Q. Z. Dai, Y. J. Xia, C. Sun, M. L. Weng, J. Chen, J. D. Wang and J. M. Chen, *Chem. Eng. J.*, 2014, **245**, 359–366.
15 F. D. A. de Figueredo-Sobrinho, F. W. D. Lucas, T. P. Fill, E. Rodrigues, L. H. Mascaro, P. N. D. Casciano, P. de Lima-Neto and A. N. Correia, *Electrochim. Acta*, 2015, **154**, 278–286.
16 X. Li, D. Pletcher and F. C. Walsh, *Chem. Soc. Rev.*, 2011, **40**, 3879–3894.
17 Y. Yao, M. Zhao, C. Zhao and H. Zhang, *Electrochim. Acta*, 2014, **117**, 453–459.
18 Y. W. Yao, M. M. Zhao, C. M. Zhao and X. Wang, *J. Electrochem. Soc.*, 2013, **160**, D553–D557.
19 I. Sirés, C. T. J. Low, C. Ponce-de-León and F. C. Walsh, *Electrochem. Commun.*, 2010, **12**, 70–74.
20 I. Sirés, C. T. J. Low, C. Ponce-de-León and F. C. Walsh, *Electrochim. Acta*, 2010, **55**, 2163–2172.
21 Z. Hu, M. Zhou, L. Zhou, Y. Li and C. Zhang, *Environ. Sci. Pollut. Res. Int.*, 2014, **21**, 8476–8484.
22 K. Pan, M. Tian, Z. H. Jiang, B. Kjartanson and A. C. Chen, *Electrochim. Acta*, 2012, **60**, 147–153.
23 M. Cerro-Lopez, Y. Meas-Vong, M. A. Méndez-Rojas, C. A. Martínez-Huitle and M. A. Quiroz, *Appl. Catal., B*, 2014, **144**, 174–181.
24 Y. Jiang, Z. Hu, M. Zhou, L. Zhou and B. Xi, *Sep. Purif. Technol.*, 2014, **128**, 67–71.
25 O. Shmychkova, T. Luk'yanenko, A. Yakubenko, R. Amadelli and A. Velichenko, *Appl. Catal., B*, 2015, **162**, 346–351.
26 O. Shmychkova, T. Luk'yanenko, A. Velichenko, L. Meda and R. Amadelli, *Electrochim. Acta*, 2013, **111**, 332–338.

 This journal is © The Royal Society of Chemistry 2016

Published on 07 January 2016. Downloaded by Xian Jiaotong University on 11/08/2016 08:26:43.

27 X. Hao, L. Jingjing, Y. Wei and C. Wei, *Rare Met. Mater. Eng.*, 2013, **42**, 885–890.
28 H. Lin, J. Niu, J. Xu, Y. Li and Y. Pan, *Electrochim. Acta*, 2013, **97**, 167–174.
29 Q. Li, Q. Zhang, H. Cui, L. Ding, Z. Wei and J. Zhai, *Chem. Eng. J.*, 2013, **228**, 806–814.
30 J. F. Niu, H. Lin, J. L. Xu, H. Wu and Y. Y. Li, *Environ. Sci. Technol.*, 2012, **46**, 10191–10198.
31 Y. W. Yao, T. Zhou, C. M. Zhao, Q. M. Jing and Y. Wang, *Electrochim. Acta*, 2013, **99**, 225–229.
32 Y. Yao, C. Zhao and J. Zhu, *Electrochim. Acta*, 2012, **69**, 146–151.
33 X. Hao, S. Dan, Z. Qian, Y. Honghui and Y. Wei, *RSC Adv.*, 2014, **4**, 25011–25017.
34 F. W. Wang, S. D. Li, M. Xu, Y. Y. Wang, W. Y. Fang and X. Y. Yan, *J. Electrochem. Soc.*, 2013, **160**, D53–D59.
35 Q. Dai, H. Shen, Y. Xia, F. Chen, J. Wang and J. Chen, *Sep. Purif. Technol.*, 2013, **104**, 9–16.
36 H. S. Kong, W. Li, H. B. Lin, Z. Shi, H. Y. Lu, Y. Y. Dan and W. M. Huang, *Surf. Interface Anal.*, 2013, **45**, 715–721.
37 X. Hong, R. Zhang, S. Tong and C. A. Ma, *Chin. J. Chem. Eng.*, 2011, **19**, 1033–1038.
38 L. S. Andrade, R. C. Rocha-Filho, N. Bocchi, S. R. Biaggio, J. Iniesta, V. Garcia-Garcia and V. Montiel, *J. Hazard. Mater.*, 2008, **153**, 252–260.
39 L. Zhang, L. Xu, J. He and J. Zhang, *Electrochim. Acta*, 2014, **117**, 192–201.
40 X. Duan, F. Ma, Z. Yuan, L. Chang and X. Jin, *Electrochim. Acta*, 2012, **76**, 333–343.
41 X. Duan, F. Ma, Z. Yuan, L. Chang and X. Jin, *J. Electroanal. Chem.*, 2012, **677–680**, 90–100.
42 P. Ju, H. Fan, D. Guo, X. Meng, M. Xu and S. Ai, *Chem. Eng. J.*, 2012, **179**, 99–106.
43 W. Yang, W. Yang and X. Lin, *Appl. Surf. Sci.*, 2012, **258**, 5716–5722.
44 S. P. Tong, C. A. Ma and H. Feng, *Electrochim. Acta*, 2008, **53**, 3002–3006.
45 S. Ghasemi, M. F. Mousavi and M. Shamsipur, *Electrochim. Acta*, 2007, **53**, 459–467.
46 L. Ciríaco, C. Anjo, J. Correia, M. J. Pacheco and A. Lopes, *Electrochim. Acta*, 2009, **54**, 1464–1472.
47 H. Bi, C. Yu, W. Gao and P. Cao, *Electrochim. Acta*, 2013, **113**, 446–453.
48 H. An, Q. Li, D. Tao, H. Cui, X. Xu, L. Ding, L. Sun and J. Zhai, *Appl. Surf. Sci.*, 2011, **258**, 218–224.
49 F. Montilla, E. Morallon and A. D. B. J. L. Vazquez, *J. Phys. Chem. B*, 2004, **108**, 5036–5043.
50 H. S. Kong, H. Y. Lu, W. L. Zhang, H. B. Lin and W. M. Huang, *J. Mater. Sci.*, 2012, **47**, 6709–6715.